Journal of Aeronautics and Space Technologies

17(2) (2024) 107-121

Journal Homepage: jast.hho.msu.edu.tr

RESEARCH ARTICLE

Numerical Study of 2D Curved Shock Wave Turbulent Boundary Layer Interaction

İki Boyutlu Kavisli Şok Dalgası Türbülanslı Sınır Tabaka Etkileşiminin Sayısal İncelenmesi

Vishal Umapathi Choudhari[1*], Keerthi J S[1], Gopalakrishna N[1]

[1] *Department of Automotive and Aeronautical Engineering, M S Ramaiah University of Applied Sciences, Bengaluru, India 560058.*

Received: *January 25, 2024* ***Revised:*** *March 29, 2024* ***Accepted:*** *June 4, 2024*

Abstract

The shock wave boundary layer interaction (SWBLI) due to curved shock is studied prominently, as most military aircrafts and missiles undergo strong SWTBLI due to its curved or blunt shape. These interactions effect the performance of vehicles at supersonic flow regime. The present numerical study investigates, interaction between a shock wave and turbulent boundary layer (SWTBLI) for cylindrical shock generators at freestream Mach number 3. The diameter (D) of cylindrical shock generator is varied to determine the effect of strength of shock on boundary layer and effect on impinging location from leading edge of flat plate, which depends upon the position of cylindrical shock generator. Two dimensional numerical simulations are carried out on mentioned model using commercially available CFD solver that employs k-omega SST turbulence model. Computational results show a good agreement qualitatively in terms of separation location and separation bubble length and quantitatively predicts the surface pressure, accurately as compared to the experiments conducted by literature.

Keywords: Shock Wave, Shock Wave/Boundary Layer Interaction, Diameter of Cylinder, Boundary Layer, Separation Bubble and Surface Pressure

Öz

Çoğu askeri uçak ve füze, kavisli ve küt şekli nedeniyle güçlü şok dalgası sınır tabakasına etkileşimine maruz kaldığından, şok dalgası sınır tabakası etkileşimi belirgin bir şekilde incelenmiştir. Bu etkileşimler araçların süpersonik akış rejimindeki performansını etkilemektedir. Bu sayısal çalışma, serbest akış Mach sayısı 3'te silindirik şok jeneratörleri için şok dalgası ve türbülanslı sınır tabaka (SWTBLI) arasındaki etkileşimi araştırmaktadır. Silindirik şok üretecinin çapı (D), şokun gücünün sınır tabaka üzerindeki etkisini ve silindirik şok üretecinin konumuna bağlı olarak düz plakanın ön kenarından çarpma konumu üzerindeki etkisini belirlemek için değiştirilmiştir. İki boyutlu sayısal simülasyonlar, k-omega SST türbülans modelini kullanan piyasada mevcut CFD çözücüsü kullanılarak söz konusu model üzerinde gerçekleştirilmiştir. Hesaplama sonuçları, literatürdeki deneylerle karşılaştırıldığında, ayırma konumu ve ayırma kabarcığı uzunluğu açısından niteliksel olarak iyi bir uyum göstermekte ve yüzey basıncını niceliksel olarak doğru bir şekilde tahmin etmektedir.

Anahtar Kelimeler: Şok Dalgası, Şok Dalgası/Sınır Tabaka Etkileşimi, Silindir Çapı, Sınır Tabaka, Ayrılma Kabarcığı ve Yüzey Basıncı

*Corresponding Author
E-mail: vishalchoudhari104@gmail.com

1. INTRODUCTION

Shock wave boundary layer interaction is widely studied in high-speed communities due to its huge impact on the aerodynamics and propulsion aspects of the vehicle. Occurrence of the SWBLI may deteriorate the aerodynamic efficiency of the control surface and structural integrity of the vehicle. The effect is more pronounced primarily in supersonic and hypersonic regime.

Numerous investigations have been undertaken to explore shock wave boundary layer interaction (SWBLI), with pioneering efforts initiated by Ferri [2]. Ferri's study, conducted on flow over a transonic airfoil, marked the inception of research into this complex phenomenon. In the mid-1940s, Fage, Sergent, and Ackeret [3] delved into SWBLI at transonic speeds, highlighting the inherent challenges in systematically examining its properties. Subsequent computational studies were conducted by Knight and Degrez [4], focusing on the SWBLI of double fin, single fin, and hollow cylinder flare configurations. The outcomes of these studies indicated that predictions for the laminar case were accurate, while challenges emerged in modeling turbulent case due to intricate nature of triple deck within the boundary layer. The present study focuses on capturing SWBLI phenomena with the turbulent boundary layer using available computational resources.

The shock wave boundary layer interaction is classified as weak interaction and strong interaction. Weak interaction is where the outer inviscid flow and resulting shock patterns are weakly altered. Conversely, strong interaction involves a pronounced coupling between the inviscid and viscous components of the flow field, resulting in formation of a separation bubble. The adverse pressure induced separation is the primary phenomenon of SWBLI, shock is the secondary associated artifact. In the context of viscous flow, separation of boundary layer remains consistent with incompressible flow. The primary flow characteristics persist in both laminar and turbulent conditions, with the differentiating factor lying in magnitude of interaction, specifically pressure loads. The interaction zone can be several times greater than its corresponding turbulent case for same overall pressure rise. Furthermore, it has been observed that altering the impingement location under constant shock strength results in an increase in boundary layer thickness and, consequently, formation and increase in the separation bubble size.

SWBLI phenomena as observed in Figure 1, shock from the shock generator impinges on flat plate till the inner part of boundary layer. The adverse pressure gradient from the shock leads to separation of boundary layer. This is denoted by the formation of separation shock. The total length of separation is denoted as Lsep which is the distance from the point of separation, till reattachment point. Separation shock C2 interacts with impinging shock C1 which gets transmitted as oblique shocks C3 and C4. This interaction points between the impinging shock C1, separation shock C2 and shock C3 is referred as triple point, I.

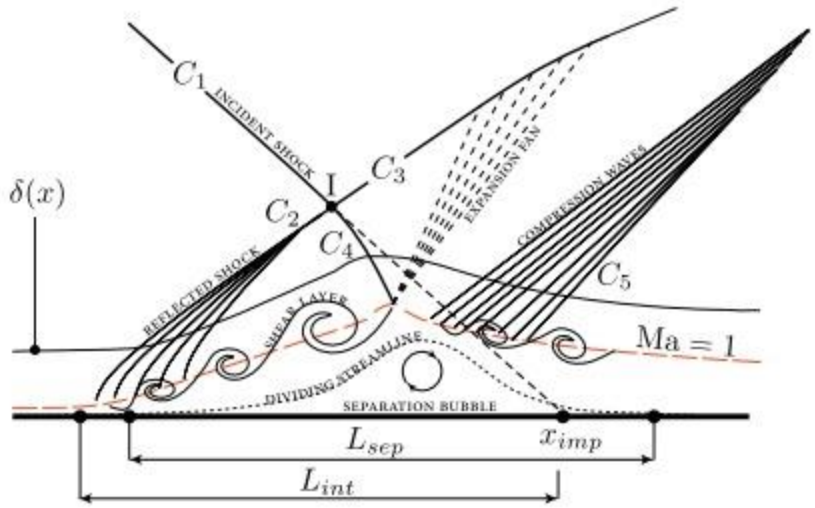

Figure 1. Schematic depicting the flow phenomena of impinging SWBLI [1].

Flow adjacent to the wall stagnates at the separation point. Shock C4 penetrates boundary layer till the sonic line where it further gets reflected as expansion waves. Then, reattachment shock C5 is formed due to redirection of flow along the wall. The phenomenon of shock impingement and the interactions associated with it, remains same for different kind of shock generators i.e., wedge or cylinder. This interaction involving complex phenomenon is termed as strong interaction.

In the current study impinging shock model with cylindrical shock generators has been considered due to its inherent complexities, establishing it as the standard case for investigation into separation bubble size and its correlation with the distance from leading edge. The impinging SWBLI has been studied for freestream Mach number 3 and cylindrical shock generators of two different diameters i.e., 15 mm and 30mm. Grid independence study has been carried out for surface pressure. Presently the comparison between the surface pressure is considered for varying Δx (249mm and 309mm) and Δy/D (6.67 and 3.33). Surface pressure has been validated for above mentioned parameters due to availability of experimental results [6] for comparison with computational results.

The numerical investigation yields valuable insights into the variation of surface pressure in supersonic conditions with respect to the specified parameters and sheds light on their impact on separation bubble length. Furthermore, it also helps to validate the ability of turbulence model used to obtain results and accurately capturing the phenomena associated with the separation bubble such as separation shock, reattachment shock, expansion fans and similar intricacies.

2.GEOMETRIC AND NUMERICAL DETAILS

2.1 Geometric Details

The experimental study was conducted by Touré, P.S. and Schülein [6], in DLR German aerospace center for impinging SWBLI. The varying diameter cylinders were considered

as shock generators. Exchangeable spacers were used to change the location of cylinders from leading edge of the flat plate. The tests were conducted in Ludwieg tube facility which covers a Mach number from 2 to 7. Along with the varying cylinder diameters, the effect of change in location of cylinder was studied. Test model used in the experiment is shown in Figure 2(a). The flat plate with sharp leading edge has total length of 670mm. In the present study, cylindrical shock generators of two different diameters i.e., 15mm and 30mm is considered. Both are placed at same vertical distance from the flat plate at 100mm.

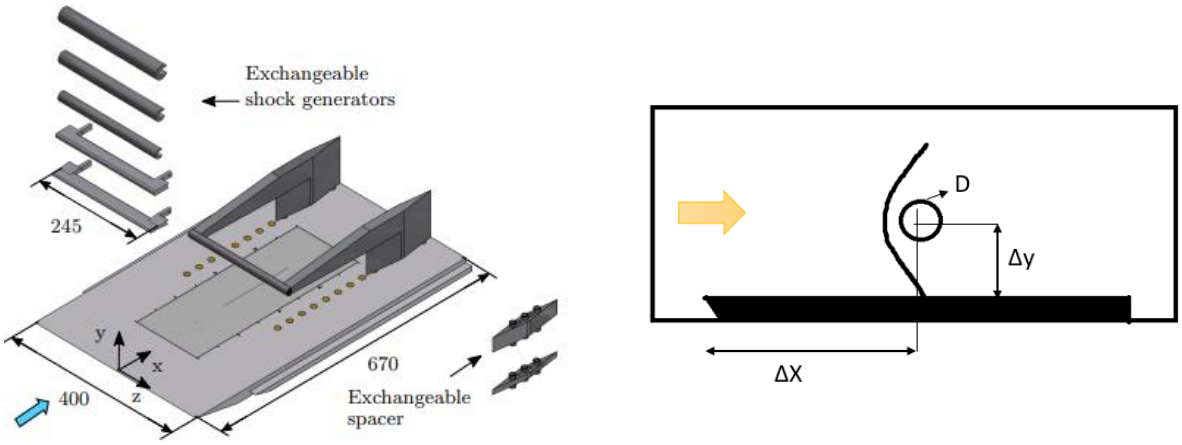

a) Test model used in the experiment **b)** 2D representation of test model

Figure 2. Geometric model and parameters associated with shock generator location for SWBLI. [6]

The simplified 2D representation of the domain along with cylindrical shock generator is depicted in Figure 2(b).

Table 1. Geometric dimensions of model and location of shock generator.

Case	D (mm)	Δx (mm)	Δy (mm)	$\Delta y/D$ (mm)
1	15	249	100	6.67
2	30	309	100	3.33

Two distinct cases were considered in the numerical investigation, as outlined in Table 1. In both cases, diameter of cylinder (D) , horizontal distance between the leading edge of flat plate and center of shock generator cylinder was varied i.e., Δx, whereas the vertical distance was consistently maintained at a constant value equal to 100mm.

2.2. Computational Details

Computational details and freestream conditions used for present study is discussed in this section. The parameters considered are freestream Mach number of 3, total pressure of 5.15±0.11 bar, total temperature of 266.1±2.7 K, static temperature of 263.4K and unit Reynolds number equal to 46× 10^6 m^{-1} which are tabulated in Table 2.

Table 2. Free Stream Conditions considered for computational study.

Mach Number	Static Pressure (bar)	Static temperature (K)	Reynolds number (10^6 m^{-1})
3	5.04	263.4	46

Computational domain with the specified boundary conditions is shown in Figure 3. The distance is specified according to case 1 with diameter of cylinder equal to 15mm, which is located at 249mm from the leading edge of flat plate. Structured mesh is generated using commercially available meshing tool.

Simulations were conducted using the commercially available solver ANSYS Fluent. RANS k – omega SST turbulence model has been used for validation. k-omega turbulence model, is a two-equation turbulence model used to solve turbulent kinetic energy and specific dissipation energy.

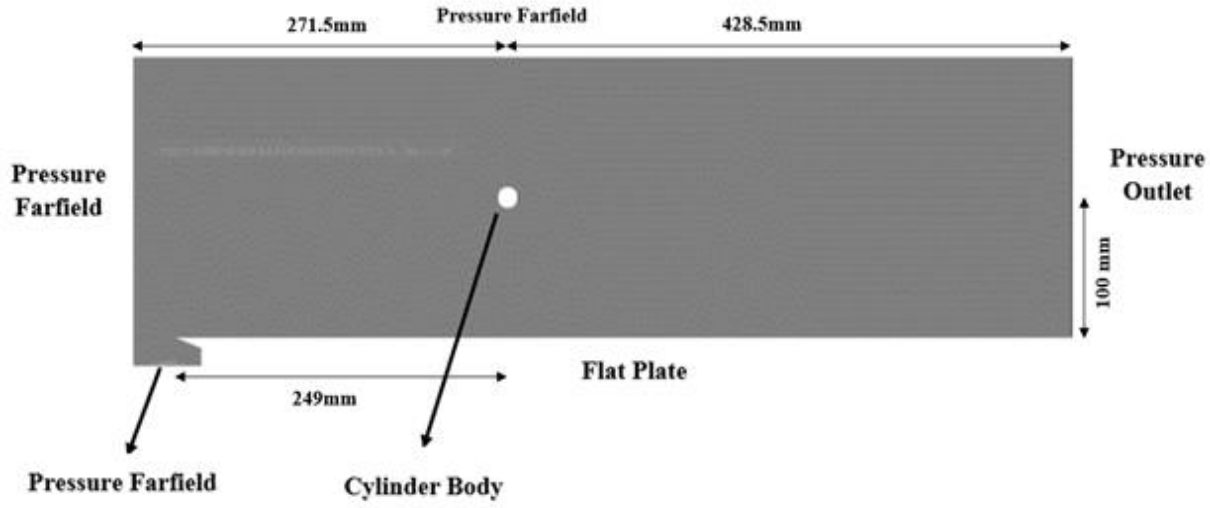

Figure 3. Computational domain with boundary conditions.

k-omega turbulence model has been employed specifically for internal flows, making it particularly useful in simulating wall-bounded flows such as boundary layer flows. This model incorporates the effects of turbulence near solid surfaces, which can significantly impact flow characteristics. Additionally, k-omega SST model is effective in predicting surface parameters. Sutherland viscosity model is considered due to temperature dependency prominently observed in high speed supersonic and hypersonic flows. Hence,

three coefficient sutherland viscosity model has been adopted. AUSM (Advection upstream splitting method) is used for inviscid flux discretization. AUSM is proved to be accurate for capturing shock and contact discontinuities with better accuracy and convergence rate for high-speed flows. Green-gauss cell-based method is considered for computing secondary diffusion and velocity derivatives, where the face values are calculated by taking mathematic average of values at neighbouring cell centers [7].

Computations were conducted with a convergence criterion set at 10^{-6}. The implemented boundary conditions are elucidated in Figure 3. Pressure far-field condition was utilized to replicate free stream conditions at infinity, with given freestream mach number and free stream conditions in Table 2. Pressure outlet is used as outlet boundary condition. Cylinder and flat plate have no-slip isothermal wall condition. The ratio of wall temperature to free stream temperature known as wall recovery temperature ratio is 0.85, and wall temperature is considered to be 287 K according to the experiments conducted [6].

3. RESULTS AND DISCUSSION

The results for SWBLI using cylindrical shock generator at freestream Mach number 3 is presented in this section. Two cases are elaborated based on the size of cylinders and location of shock impingement on the flat plate.

3.1. Grid Independence Study (GIS)

The grid independence study was conducted to determine the most appropriate grid size. In the numerical study, three distinct grid sizes coarse, medium and fine were considered of 0.2, 0.4 and 0.8 million cells, respectively.

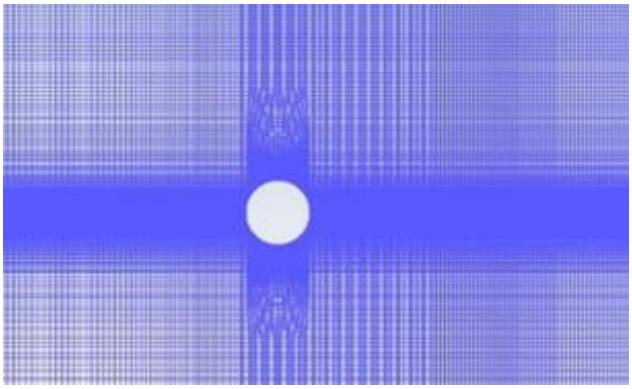

Figure 4. Mesh generated around cylindrical shock generator.

The grid size variations were implemented to maintain a grid ratio of 2. First layer spacing was calculated considering reasonable y^+ value and required number of boundary layers is used precisely capture the flow physics. The grid was specifically made fine near the wall region to accurately capture the flow associated properties, such as separation shock, separation bubble, reattachment shock and other associated surface parameters.

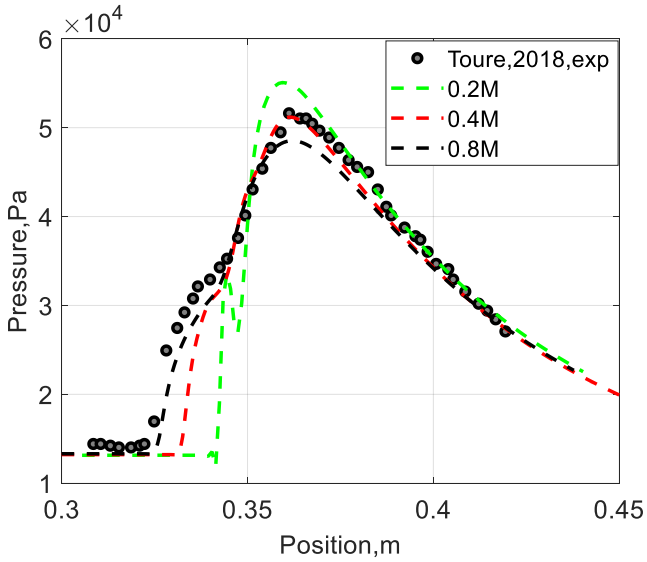

Figure 5. Wall pressure comparison of different mesh for a shock generator of diameter = 15mm located at Δx = 249mm and Δy/D is 6.67.

Figure 4 illustrates the grid spacing near cylindrical body. The grid independence study of surface pressure is indicated in Figure 5. Coarse grid does not accurately predict the start of separation. This results in underestimation of separation bubble length size and overestimation of peak pressure values. In comparison to coarse gird, medium and fine grids predict the start of separation and separation bubble size, which has a good agreement with the experimental results [6]. To obtain better prediction of results, further all computational studies have been conducted with the fine grid.

Case 1: Shock Generator of D=15mm, Location from the Leading Edge of the Plate is Δx = 249mm and Δy /D = 6.67

The cylindrical shock generator of 15mm, induces the formation of a bow shock in front of the cylinder. This bow shock upstream of the cylinder is characterized by a decreasing shock angle from 90 degrees downwards, corresponding to a reduction in the nominal shock strength which further acts as impinging shock towards flat plate.

Figure 6(a) shows the presence of bow shock in front of cylinder body. The adverse pressure gradient from shock leads to formation of separation bubble on the flat plate. It also highlights presence of separation bubble, impinging shock, separation shock and reattachment shock. Weak expansion fans are originated from the reflection of impinging shock on the shear layer.

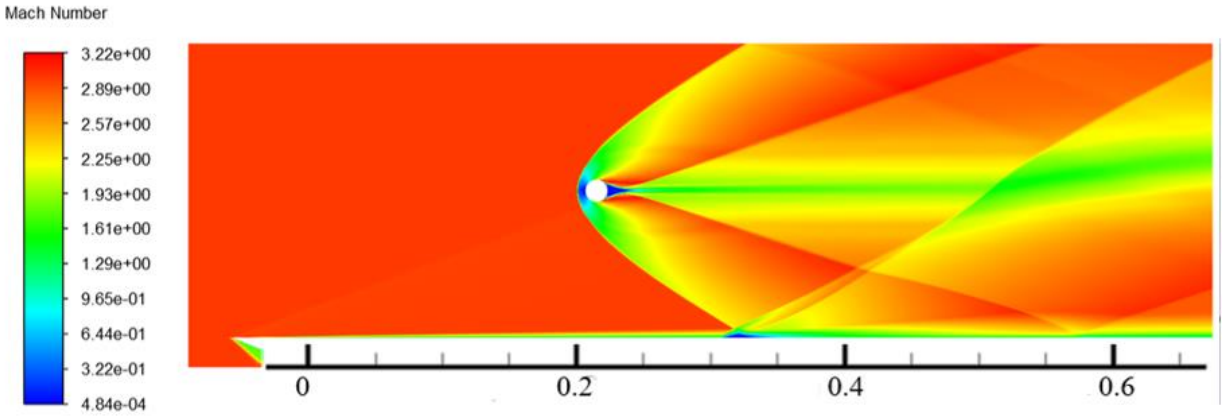

a) Mach contour for Case 1

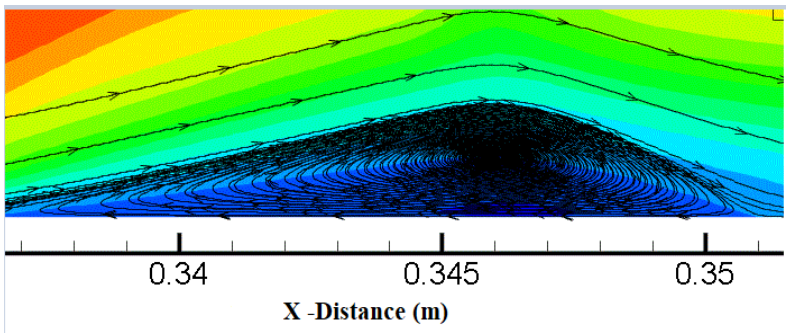

b) Streamline plot near separation bubble region

Figure 6. Mach Contour and streamline plot at the separation bubble for shock generator (D) of 15mm, located at $\Delta x = 249$mm and $\Delta y/D = 6.67$.

Furthermore, streamlines of freestream mach number, indicating the presence of a recirculation bubble is observed in Figure 6 (b). The near view of separation bubble shows the location of start of the recirculation and end of the recirculation bubble with the help of streamlines.

In Figure 7(a), density contour near separation bubble obtained from numerical investigation results can be observed. Qualitatively, the obtained results exhibit good agreement with experimental shadowgraph results as illustrated in Figure 7(b). It illustrates that the k-Omega turbulence model, coupled with AUSM scheme, is capable of qualitatively capturing the flow phenomena associated with curved Shock Wave Boundary Layer Interaction (SWBLI). Figure 7(b) shows the shadowgraph image from the wind tunnel tests where boundary layer thickness increases across the length of the flat plate.

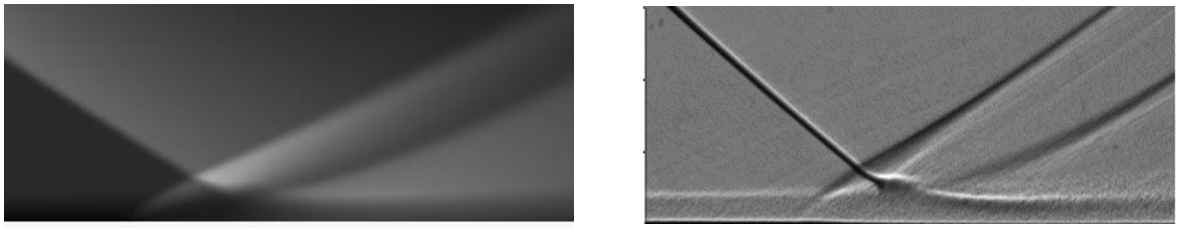

a) Shadowgraph image from computational study for Case 1

b) Shadowgraph image from the Experiment for Case 1

Figure 7. Comparison of numerical and experiment shadowgraph for a SWTBLI for mach number of 3. [6]

As the thickness further increases, owing to adverse pressure gradients, it leads to the separation of boundary layer, which subsequently reattaches, resulting in the formation of a recirculation bubble. This phenomenon is accurately captured with the help of computational study.

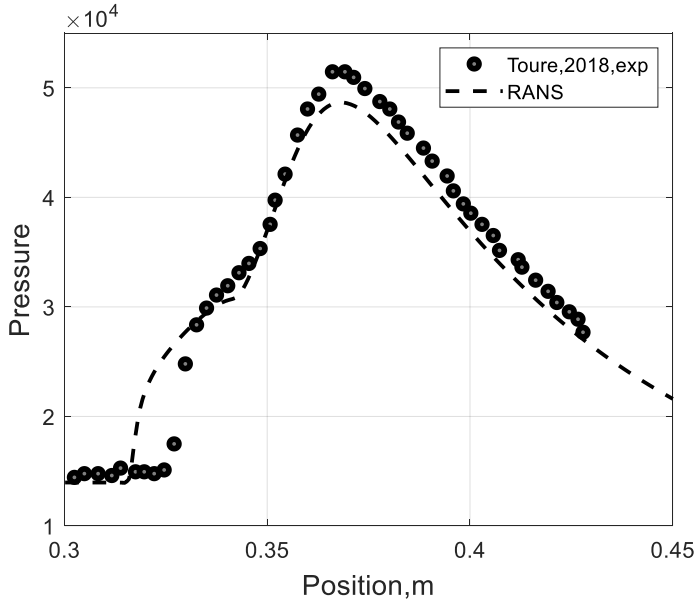

Figure 8. Validation of surface pressure distribution for shock generator diameter of 15mm, located at Δx = 249mm and Δy/D = 6.67.

In present case, with a Δy/D ratio of 6.67, Figure 8 illustrates surface pressure distribution plot that clearly depicts the adverse pressure gradient induced by bow shock, leading to formation of a separation bubble on flat plate. Positioned at a vertical distance of 100mm from the centre of cylinder with a diameter of 15mm, flat plate exhibits separation starting at location denoted as S (x=336mm). Surface pressure distribution on the flat plate is segmented by a pressure plateau at x=340mm, where pressure rise is equal to 32000Pa. The rise in pressure at location of x=336mm is attributed to separation and is associated with the separation shock C2, indicating the initial compression [8].

Subsequently, at the location of x=350mm, there is a pressure increase due to compression at reattachment which is associated with the reattachment shock C5. At the reattachment location of separation bubble, a maximum pressure of 52000Pa has been obtained. This elevation in pressure is a result of momentum transfer from inviscid part of flow field into the separation bubble, leading to high pressure at reattachment location and flow reattaches itself to the main flow after reattachment location. The numerical study is able to accurately predict the rise in pressure due to the separation bubble and the numerical results are in agreement with experimental results.

Case 2: Shock Generator of D=30 mm, Location from the Leading Edge of the Plate is Δx = 309 mm and Δy /D = 3.33

The diameter of cylinder is increased from 15mm to 30mm in Case 2. This augmentation in diameter results in the formation of a stronger shock. As diameter is increased, strength of the bow shock intensifies, leading to a larger separation bubble size illustrated in Figure 9(a).

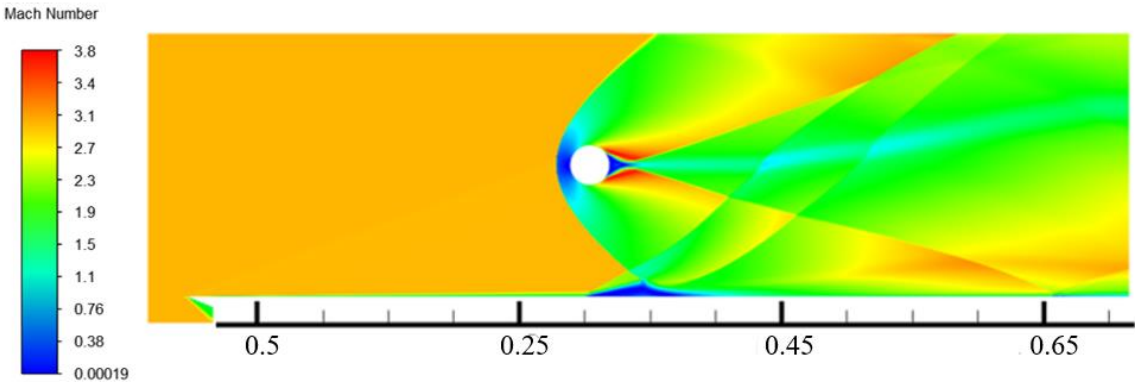

a) Mach contour for Case 2

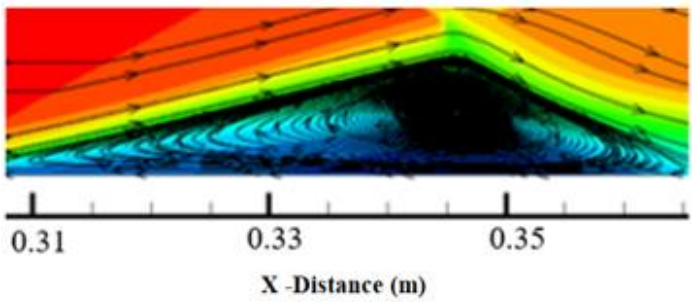

b) Streamline plot near separation bubble region

Figure 9. Mach Contour and streamline plot at the separation bubble for shock generator (D) of 30 mm, located at Δx = 309mm and Δy/D = 3.33.

Higher shock strength, resulting from increased diameter of cylinder, induces an adverse pressure gradient, contributing to the formation of a larger separation bubble as illustrated in Figure 9 (b).

Figure 9 (b) shows near view of separation bubble, clearly indicating an increased length in Case 2 compared to Case 1. This observation is further supported by surface pressure distribution graph.

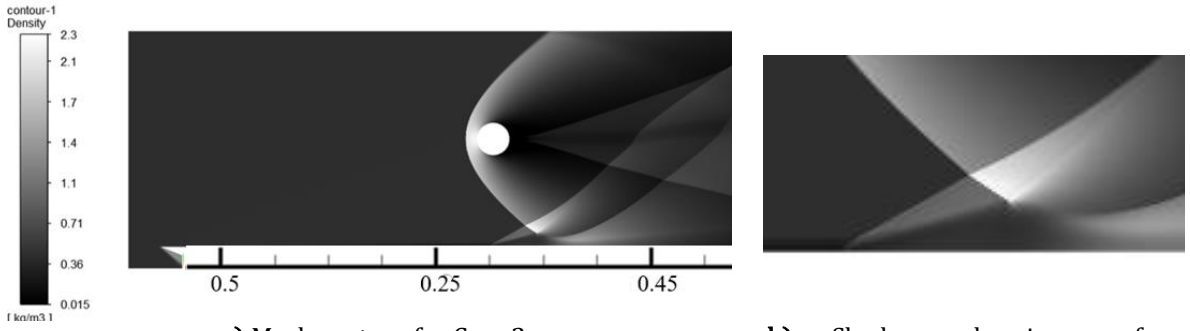

a) Mach contour for Case 2

b) Shadowgraph image from computational study for Case 1

Figure 10. Density Contour and streamline plot at the separation bubble for shock generator diameter of 30 mm, located at $\Delta x = 309$mm and $\Delta y/D = 3.33$.

Figure 10 (a) presents the density contour obtained from numerical investigation. Similarly, Figure 10 (b) illustrates density contour near separation bubble, of the same. Separation bubble length is increased due to higher shock strength of the impinging shock generated from cylinder of diameter of 30 mm.

In present Case, Δy/ D ratio is 3.33, and horizontal distance i.e. Δx is varied from 249mm to 309mm.Δy/D ratio is decreased by half in this scenario and impact of these parameter changes is investigated. This alteration in shock impingement location prompts the onset of separation bubble at x=310mm.

At location of x=310mm in Case 2, pressure increases due to the presence of separation shock C2. The pressure plateau is marked at 37000 Pa, representing a 15% increase compared to Case 1. The peak pressure at 360mm is attributed to reattachment compression waves with the value around 75000 Pa. This peak pressure is elevated by 42.4% in case 2 when compared to case 1.

Shock strength and boundary layer thickness play crucial roles in the formation of separation bubble. The thickness of boundary layer is a key factor influencing the size of separation bubble, where an increase in boundary layer thickness corresponds to an enlargement of separation bubble.

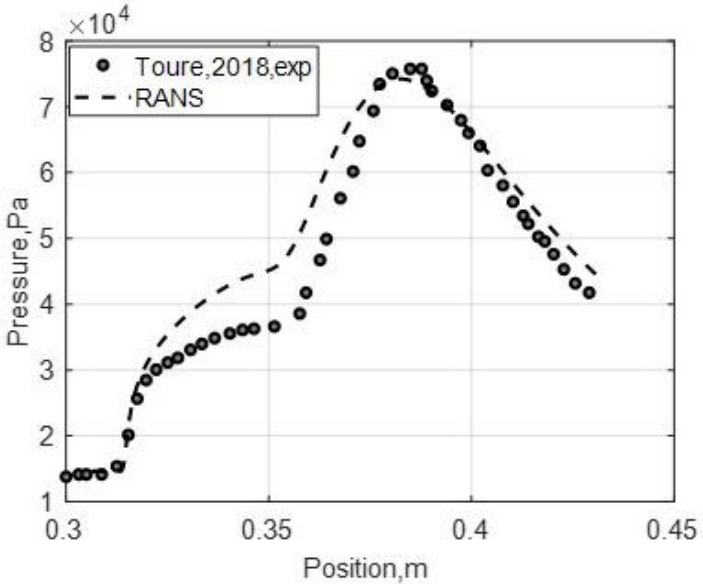

Figure 11. Surface Pressure Distribution for shock generator diameter of 30mm, located at $\Delta x = 309$mm and $\Delta y/D = 3.33$.

In Case 1, for a horizontal distance (Δx) of 249mm, thickness of boundary layer just before separation is measured to be 2.4mm. This leads to separation and later the boundary layer thins out. The interaction between the shock and boundary layer induces changes in the boundary layer thickness, ultimately contributing to the development of separation bubble.

Table 3. Flow parameters obtained from SWTBLI simulations for freestream mach number 3.

	Distance Δx(mm)	BL thickness before separation(mm)	S(mm)	R(mm)	Lsep(mm)
Case 1	249	2.4	336.5	350.1	13.6
Case 2	309	5.4	310	360	50

Similarly in Case 2, for a horizontal distance(Δx) is 309mm, boundary layer thickness just before separation at $x = 310$ mm is measured to be 5.4mm. Boundary layer thickness is increased due to influencing parameters such as change in impinging shock distance, shock strength and diameter of cylinder. As the boundary layer thickness is increased from case 1 to case 2, separation bubble length is also increased.

3.2. Comparison Between Surface Pressure, Δx and Δy/D:

The decrease in ratio of Δy/ D and change in impinging shock distance leads to a 42.4% rise in wall pressure. This increment can be attributed to enlarged separation bubble size, evident in surface pressure comparison plot in Figure 12. Two different Δx values have been considered i.e 249mm and 309mm, with a difference of 60mm. This deliberate

variation facilitates the comparison of shock impingement locations and the analysis of changes in boundary layer thickness with alteration in the impingement location.

As the distance Δx is altered from 249mm to 309mm, and increase in the diameter of cylinder, there is a 55.5% increase in boundary layer thickness. In Case 2, shock impinges on flat plate at a nearer location from leading edge compared to Case 1. This is due to increase in shock impingement angle for case 2 as diameter of cylinder is doubled in size. As the shock angle is increased with respect to cylinder, impingement of shock on flat plate is further ahead in Case 2.

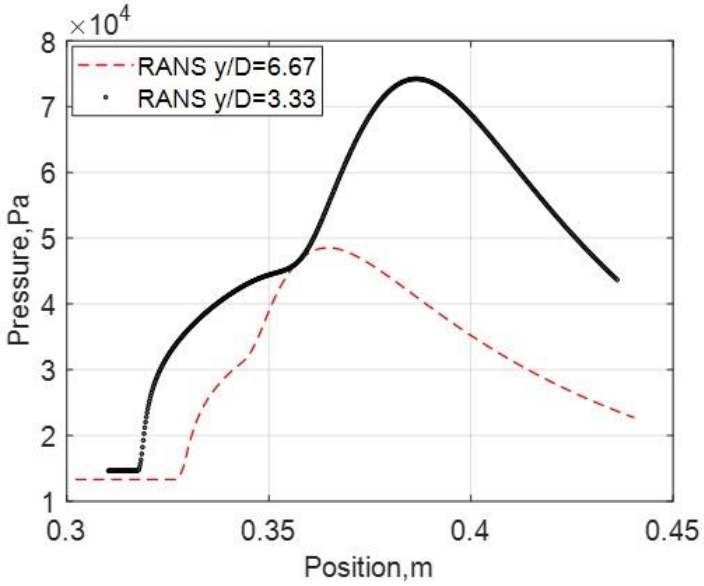

Figure 12. Surface pressure distribution comparison of shock generator diameter of 15 mm and 30 mm located at Δx = 249 mm and 309mm respectively.

The change in cylinder diameter from D=15mm to D=30mm results in an expansion of subsonic region leading to formation of compression waves. The formation of these compression waves in the Case 2 is at 310mm, whereas in Case 1, the compression waves are formed at 336m and the onset location of separation bubble increases as the diameter increases. This alteration aligns with the fundamental bow shock topology.

The length of the separation bubble is observed to vary as the diameter of cylinder is increased from 15mm to 30mm, a distinction clearly visible in Figures 6(b) and 9 (b). Table 3 provides the specific lengths of the separation bubble for both cases.

4. CONCLUSION

The present study focuses on SWBLI using a cylindrical shock generator of varying diameter and horizontal distance. The primary focus is predicting surface pressure at freestream Mach number 3, considering two distinct shock generator locations of Δx=249 mm, Δy/D= 6.67 and Δx=309 mm, Δy/D= 3.33 from leading edge, in turn varying the separation bubble size and location of start of separation.

The comparison between the numerical results and experimental data [6] reveals a good agreement in terms of surface pressure, demonstrating the model's capability to accurately capture this complex flow physics.

The separation location is approximately well predicted by CFD solver. For Case 1 i.e. shock generator diameter of 15 mm, located at $\Delta x = 249$ mm and $\Delta y/D = 6.67$. The separation location is 336.5mm, which is approximately equal to the separation location given by the experimental results from wind tunnel tests. For case 2 i.e. shock generator diameter of 30 mm, located at $\Delta x = 309$ mm and $\Delta y/D = 3.33$, separation starts at a location of 310 mm which is very well predicted by the numerical study. Similarly, thickness of boundary layer is measured to be 2.4 mm and 5.4 mm for case 1 and case 2 respectively. Separation bubble length size is 13.6 mm and 50 mm for case 1 and case 2 respectively.

The cylindrical shock generator varies in diameter, with values of 15 mm and 30 mm. This increase in diameter increases the shock strength resulting in 42.4% increase in surface pressure. The effect on boundary layer thickness is increased around 55.5% when distance from leading edge of flat plate to shock generator is increased by 60mm and diameter is increased by factor 2.

The current study exclusively employs k-omega turbulence model. Future research endeavors will delve into a comprehensive computational study incorporating various turbulence models, facilitating the identification of a more suitable turbulence model for subsequent investigations. Further study on varying cylindrical shock generator diameters is essential for a comprehensive understanding of flow phenomena associated with curved shock wave boundary layer interaction (SWBLI). Investigating the unsteady effects related to separation bubble due to upstream influence is crucial, as these effects contribute substantially to efficiency decrease observed in supersonic vehicles. Recognizing the challenges in surface pressure and separation bubble prediction, future work is aimed at a more detailed study and validation in various aspects, such as turbulence modeling and high-fidelity computational approaches.

REFERENCES

[1] Pasquariello, V., Grilli, M., Hickel, S. and Adams, N.A., 2014. *Large-eddy simulation of passive shock-wave/boundary-layer interaction control.* International Journal of Heat and Fluid Flow, **49**, pp.116-127.

[2] Ferri, A., 1940. *Experimental results with airfoils tested in the high-speed tunnel at Guidonia* (No. NACA-TM-946).

[3] Fage, A. and Sargent, R.F., 1947. *Shock-wave and boundary-layer phenomena near a flat surface.* Proceedings of the Royal Society of London. Series A. Mathematical and Physical Sciences, **190**(1020), pp.1-20.

[4] Knight, D.D. and Degrez, G., 1998. *Shock wave boundary layer interactions in high Mach number flows a critical survey of current numerical prediction capabilities*. AGARD Advisory Report Agard AR, **2**, pp.1-1.

[5] Davis, J.P. and Sturtevant, B., 2000. *Separation length in high-enthalpy shock/boundary-layer interaction*. Physics of Fluids, **12**(10), pp.2661-2687.

[6] Touré, P.S. and Schülein, E., 2018. *Numerical and experimental study of nominal 2-D shock-wave/turbulent boundary layer interactions*. In 2018 Fluid Dynamics Conference (p. 3395).

[7] Fluent, A.N.S.Y.S., 2011. Fluent 14.0 user's guide. Ansys Fluent Inc.

[8] Chapman, D.R., Kuehn, D.M. and Larson, H.K., 1958. *Investigation of separated flows in supersonic and subsonic streams with emphasis on the effect of transition* (No. NACA-TR-1356).

[9] Touré, P.S. and Schülein, E., 2017. *Study of 2-D Shock-Wave/Turbulent Boundary Layer Interaction*. In 47th AIAA Fluid Dynamics Conference (p. 4123).

[10] Babinsky, H. and Harvey, J.K. eds., 2011. *Shock wave-boundary-layer interactions* **32** Cambridge University Press.

[11] Sandham, N.D., 2011. *Shock-wave/boundary-layer interactions*. NATO Research and Technology Organization (RTO)–Educational Notes Paper, RTO-EN-AVT-195.

[12] Murphree, Z.R., Combs, C.S., Wesley, M.Y., Dolling, D.S. and Clemens, N.T., 2021. *Physics of unsteady cylinder-induced shock-wave/transitional boundary-layer interactions.* Journal of Fluid Mechanics, 918, p. A39.

[13] Scaling for steady and traveling shock wave/turbulent boundary layer interactions, Toure, 2020.

To Cite This Article: Vishal Umapathi Choudhari, Keerthi J S, Gopalakrishna N, *Numerical Study of 2D curved shock wave turbulent boundary layer Interaction*, Journal of Aeronautics and Space Technologies **17**(2), 107-121 (2024).

VITAE

Vishal Umapati Choudhari received his B- Tech degree in Aerospace Engineering from Faculty of Automotive and Aeronautical Engineering, M S Ramaiah University of Applied Sciences, Bangalore, India in 2023. He is currently working at HCL Technologies Ltd. as Senior Software Engineer.

Keerthi J S received her B- Tech degree in Aerospace Engineering from Faculty of Automotive and Aeronautical Engineering, M S Ramaiah University of Applied Sciences, Bangalore, India in 2023. She is currently working at HCL Technologies Ltd. as Senior Software Engineer.

Gopalakrishna N received his Ph.D. from Department of Aerospace Engineering, Indian Institute of Science, Bangalore, India in 2019. He received his M.Sc. Engineering degree in Aerospace Engineering from Department of Aerospace Engineering, Indian Institute of Science, Bangalore, India in 2014. He received his B.E degree in Mechanical Engineering from Faculty of Mechanical Engineering, Ramaiah Institute of Technology, Bangalore, India in 2008. He is currently working at Dronevionics Pvt Ltd, Mumbai, India as Senior CFD Engineer.